Langmuir

Article

pubs.acs.org/Langmuir

Actin Filament Motility Induced Variation of Resonance Frequency and Rigidity of Polymer Surfaces Studied by Quartz Crystal Microbalance

Harm van Zalinge,[†] Jenny Aveyard,[†] Joanna Hajne,[†] Malin Persson,[‡] Alf Mansson,[‡] and Dan V. Nicolau*,[†]

[†]Department of Electrical Engineering and Electronics, University of Liverpool, Brownlow Hill, Liverpool, L69 3GJ, United Kingdom

[‡]School of Natural Sciences, Linnaeus University, SE-39245 Kalmar, Sweden

ABSTRACT: This contribution reports on the quantification of the parameters of the motility assays for actomyosin system using a quartz crystal microbalance (QCM). In particular, we report on the difference in the observed resonance frequency and dissipation of a quartz crystal when actin filaments are stationary as opposed to when they are motile. The changes in QCM measurements were studied for various polymer-coated surfaces functionalized with heavy meromyosin (HMM). The results of the QCM experiments show that the HMM-induced sliding velocity of actin filaments is modulated by a combination of the viscoelastic properties of the polymer layer including the HMM motors.

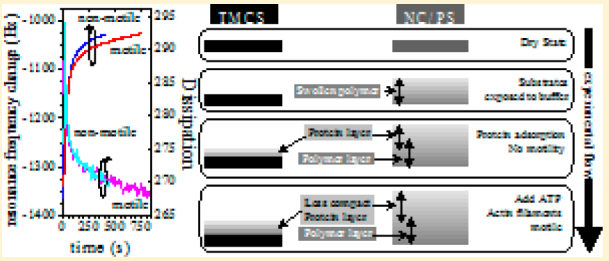

1. INTRODUCTION

The mechanical work at the nanoscale in biological systems is performed by a variety of force-generating biomolecules, among which the linear protein molecular motors, comprising myosins,[1,2] kinesins,[3−5] and dyneins,[6,7] are of extreme importance, involved in critical biological processes as diverse as cell division to neuronal transmission and cancer processes. One of the examples of force generation is muscle contraction, which is powered by the actin−myosin system through the ATP-driven translocation of actin filaments by the myosin II motors.[8,9] The development of the in vitro motility assay in the 1980s allowed the visualization of actomyosin motility, either as myosin-coated fluorescent beads moving over surface-bound actin filaments[10,11] or more commonly as fluorescently labeled actin filaments moving over a layer of surface-bound myosin.[12] The latter type of motility assay has since been used extensively to study the fundamentals of molecular motor function.[13−15] From an applications perspective, the ability of motor proteins to transport nanoscale loads, at speeds that are several orders of magnitude larger than those caused by molecular diffusion, opens up a wide range of applications in engineered nanodevices.[16,17] Among the several possible uses of the actomyosin system, an important application would be the shortened response time of biosensing devices.[18] For the better-described kinesin−microtubules system, various uses of molecular motors have also been demonstrated, from directed transport for molecular scale assembly,[19] microfluidic pumping,[19] to the movement of microsized silicon chips.[20]

In a conventional in vitro motility assay, the motor protein is adsorbed on a surface (typically nitrocellulose), and the filaments are propelled by the surface-bound motor protein upon the addition of ATP in the motility assay flow cell. The demonstration of more advanced molecular motor-based devices will require the control of both the location and the direction of the filament motion. Surface coatings used in these studies, such as methacrylate polymers,[21−23] polyurethane,[24] plasma polymerized poly(ethylene oxide),[25] polyelectrolytes,[26] commercial photoresists,[27−31] and silane functionalization,[32,33] must be both suitable for micro/nanofabrication and allow the preservation of the molecular motor activity.

Previous studies[34,35] that used rigid and soft polymer surfaces, respectively, focused on the surface hydrophobicity the motor protein is immobilized on as the main modulator of the functionality of myosin for motility assays. These studies revealed a complex, at times contradictory, relationship between the surface hydrophobicity and motility, suggesting that other parameters modulate the motility as well, perhaps stronger than hydrophobicity alone. To this end, we used quartz crystal microbalance (QCM) methodology to study the properties of the films supporting the molecular motors and their impact on the motility characteristics, in particular the sliding velocity of actin filaments.

2. EXPERIMENTAL DETAILS

All chemicals and solvents were purchased from Sigma Aldrich unless stated.

2.1. Solutions and Functionalization of Quartz Resonators. Solutions were prepared as follows: nitrocellulose (NC) 1% (w/v) in amyl acetate; polystyrene (PS, average M_r = 200 000) 2.5% (w/v) in propylene glycol methyl ester acetate (PGMEA); trimethylchlorosilane (TMCS) 5% in chloroform. For polymer functionalization, silicon oxide coated QCM quartz crystals were sonicated in ethanol and dried

Received: July 6, 2012
Revised: August 9, 2012
Published: September 18, 2012

Published 2012 by the American Chemical Society

dx.doi.org/10.1021/la302717y | *Langmuir* 2012, 28, 15033−15037

under a nitrogen flow before they were spin coated with the polymer solutions at 3600 rpm for 2 min. The crystals were subsequently baked at 85 °C for 3 h. For TMCS functionalization, the crystals were soaked in dry acetone and subsequently in chloroform for 5 min each and then exposed to TMCS vapor at 85 °C for 1 h.

2.2. Buffers for Motility. B15 comprises 1 mM $MgCl_2$, 10 mM MOPS, and 0.1 mM K_2EGTA at pH 7.4. B65 comprises B15 containing 50 mM KCl and 10 mM DTT.

2.3. Solutions for Motility Experiments. The assay solution comprises 1 mM MgATP, 10 mM DTT, 25 mM KCl, B15 with an antibleach mixture containing 3 mg/mL glucose, 20 units/mL glucose oxidase, and 870 units/mL catalase, and ATP regenerating system containing 2.5 mM creatine phosphate and 56 units/mL creatine kinase. The blocking solution comprises 1 mg/mL bovine serum albumin (BSA) in B15 buffer. The labeled actin comprises 10 μL of rhodamine phalloidin labeled actin filaments (rhodamine phalloidin was purchased from Invitrogen, and actin was labeled according to the manufacturers protocol) and 990 μL of B65. The blocking actin comprises 14 μL of unlabeled actin filaments and 986 μL of B65.

2.4. QCM Procedure. Heavy meromyosin (HMM; 600 μL of 120 μg/mL in B65) was applied to a flow cell containing the functionalized crystal and incubated for 600 s. At the end of this period, unreacted binding sites on the crystal were blocked using BSA by applying 1 mL of blocking solution to the flow cell. Following incubation for 300 s, the blocking solution in the flow cell was replaced with 1 mL of blocking actin (to block nonfunctioning HMM heads). After 120 s of incubation, excess blocking actin was removed by flushing the flow cell with 2 mL of B65, and then 1 mL of labeled actin was applied for 600 s. At the end of this time, excess labeled actin was removed by flushing the flow cell with 2 mL of B65, and 1 mL of assay solution was applied. In general, the timings during the QCM experiments were adjusted according to the stabilization time required for the QCM to acquire a steady state. All experiments were performed at a constant temperature of 25 °C.

2.5. Equipment. A Zeiss AxioImager.M1 fitted with an Andor iXon+ EMCCD camera was used to observe standard motility assays using rhodamine phalloidin labeled actin filaments. The sliding velocity of the filaments on the various surfaces was determined using ImageJ.

The QCM experiments were performed on a QCM-Z500 from KSV Instruments Ltd. The QCM is able to measure up to the 11th harmonic and able to determine the dissipation of energy in the deposited film. The crystals have a standard resonance frequency of 5 MHz and have been coated with silicon oxide at the manufacturer, Biolin Scientific/QSense. Before use in the QCM experiments, the crystals were coated with the various substrate materials as described previously. Each of the experiments was performed at least twice. The interpretation of the QCM experiments was performed using the third harmonic. During the QCM experiments, the temperature in the resonator chamber was kept at a constant temperature, 25 °C.

3. RESULTS

3.1. Resonance Frequency and Dissipation Measured by QCM before Motility State. Two sets of experiments were run in parallel, that is, the traditional motility assay on coated glass coverslips, and QCM experiments. For both experiments, the methods have been kept identical with regard to coating procedures, solutions, and protein immobilization. The classical motility assays were used to measure the sliding velocity of the actin filaments on various coatings. In the QCM experiments, the resonance frequency and its harmonics, as well as the dissipation of energy in the absorbed film, were monitored during every step of the motility assay. Figure 1 presents an overview of a characteristic QCM result.

For QCM experiments involving rigid films, the relationship between the frequency change (Δf) and the amount of mass deposited on the quartz electrode is given by the Sauerbrey equation:[36]

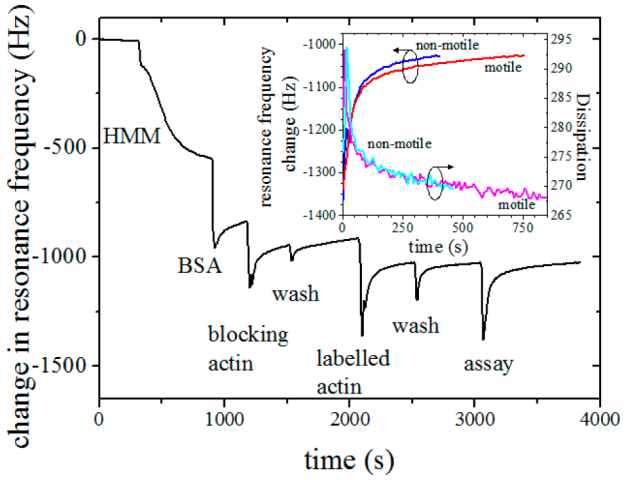

Figure 1. Change in resonance frequency (third harmonic) during a motility assay on nitrocellullose, and each separate step in the assay has been indicated. Zero change is the situation where the crystal is coated and in water. The inset shows the difference in resonance frequency and dissipation between motile (red, frequency; magenta, dissipation); 0 s in inset is 3076 s in main figure and nonmotile filaments (blue, frequency; cyan, dissipation); 0 s in inset is 2101 s in main figure. The circles and arrows indicate the relevant axis.

$$\Delta f = \frac{-2f_0^2 \Delta m}{A\sqrt{\rho_q \mu_q}}$$

where f_0 is the fundamental frequency of the crystal (5×10^6 Hz for this study), Δm is the change in mass (g), A is the electrode area (cm^2), ρ_q is the density of quartz (2.65 g cm^{-3}), and μ_q is the shear modulus of quartz (2.95×10^{11} dyn cm^{-2}). The Sauerbrey equation is only valid for rigid films, whose change in resonance frequency directly scales with the number of the harmonic. For the majority of layers used in this study, this direct scaling does not apply, and as such, they have to be treated as viscoelastic layers. Several studies have shown[37−39] that, for viscoelastic layers, the change in the resonant frequency also depends on material properties.[40,41] Moreover, for protein layers, and even more for those on supporting polymers, which are also nonrigid, the added protein layer increases both the mass loading and the energy dissipation of the QCM,[42] and this increased energy dissipation will result in an additional change in frequency over that due to mass loading alone.[43]

Under these qualifications, the first premotility steps of the motility assay yields information about the estimated amount of motors adsorbed on the crystal, as signified by the change in resonance frequency during the HMM adsorption. The adsorption of the HMM is expected to be affected by the surface coating,[44] which will ultimately lead to variation in the sliding velocity of the actin filaments. In this study, we did not look at the adsorption process itself and just used this as a given. Figure 1 presents the change in the resonance frequency for the whole duration of the motility assay procedure. This change of resonance frequency is in good agreement with previously reported QCM experiments looking at the conformation of the HMM molecule on the surface.[44]

3.2. Apparent Mass and Dissipation Measured by QCM during the Motility State. The final, during motility steps in the QCM experiments yield information about the effects of motility on the resonance frequency and dissipation.

dx.doi.org/10.1021/la302717y | Langmuir 2012, 28, 15033−15037

At a molecular level, the process of HMM propelling the filaments comprises two stages, which alternate according to different conformations of the HMM molecule.[35,44−46] In a QCM experiment, the viscoelastic properties of the adsorbed layer on the crystal will be affected by its compactness, which is in turn modulated by the conformation of the molecules composing the layer. While during the nonmotile stage of the motility assay all HMM molecules display "normal" viscoelastic properties common to all protein layers, during the motile stage, the HMM molecules will be alternating between the two, more open confirmations. The various stages of this movement of the HMM molecule correspond with the differences in the amount of water that are associated with the molecule, and this is likely to reflect in additional viscoelasticity compared with the nonmotile state, as demonstrated by the evolution of dissipation in the inset in Figure 1.

As can be seen in the inset of Figure 1 and in Table 1, a significant difference in the resonance frequency of the adsorbed film can be observed for a NC-coated crystal. Figure 2 and Table 1 present the differences in the resonance frequency and dissipation between motile and nonmotile states for the various surface coatings used (NC, TMCS, and PS) as a function of the contact angle, which is regarded as a critical parameter for the modulation of motility assay.[34,47] The values for the resonance frequency and the dissipation were determined by averaging the final points on the curves shown for example in the inset of Figure 1 for nitrocellulose. Interestingly, the difference in the resonance frequency, which as alluded above includes the effects of the change of viscoelasticity, is positive for rigid surfaces and negative for softer polymeric surfaces.

Table 1. Overview of the Used Surface Coatings and the Experimental Results

			difference between motile and nonmotile	
coating	contact angle (deg)	sliding velocity (μm/s)	resonance frequency (Hz)	dissipation
TMCS	71 ± 0.6	2.12 ± 0.11	13.0 ± 1.7	−3 ± 1
NC	70 ± 0.6	2.33 ± 0.12	−17.2 ± 1.7	0.5 ± 1
PS	77 ± 0.6	2.79 ± 0.14	−19.7 ± 1.7	7 ± 1

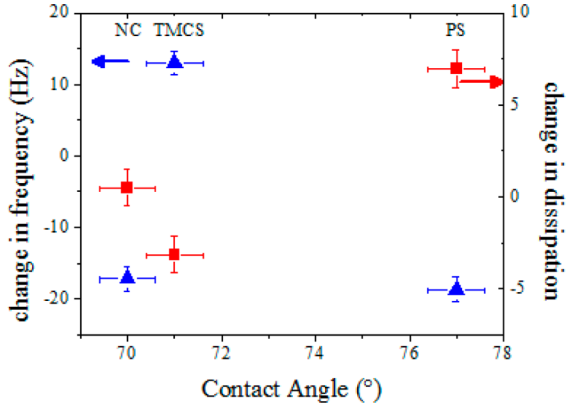

Figure 2. Difference in resonance frequency (blue triangles) and dissipation (red squares) between motile and nonmotile filaments as a function of the contact angle. The error bars represent one standard deviation. The arrows indicate the relevant axis.

The results regarding the change of QCM-measured resonance frequency are important for molecular-motor-based diagnostic devices, as they open the possibility of detecting the switch from motile to nonmotile states by means other than optical microscopy. Optical microscopy is the standard method for testing the impact of chemical species on the functioning of molecular motors in motility assays, mostly for drug discovery research.[48,49] Optical microscopy also could be the best option for other molecular-motor-based devices, where the movement of individual nano-objects needs to be recorded, such as those proposed for biosimulation.[50] However, for other applications, especially biosensing, where the overall change in motility reports an overall change in the molecular state of detecting biomolecules immobilized on surfaces, as proposed earlier,[16] optical microscopy is not the best choice as it would involve elaborate, difficult to automate image analysis procedures and as it would be difficult to implement for field applications. Conversely, QCM has been successfully applied to a large number of biosensing applications.[51,52]

Indeed, regardless of the appropriate calculation of the actual mass using complex models that account for the viscoelasticity of the film on the QCM crystal, a change in a QCM parameter following a change in the motility of the actomyosin system represents a biosensing signal transducing a change in the biomolecular state of a protein immobilized on the surface of the biosensor. Further work, which is underway, will refine this approach through factoring in the viscoelastic properties of the film, which is expected to increase the sensitivity of sensing of motility state.

3.3. Actomyosin Velocity Is Modulated by the Viscoelasticity of the Film. Aside from the on−off detection of the actin−myosin motility state, the correlation of a continuous motility parameter, such as sliding velocity, with the properties of the surface would progress the design of appropriate surfaces for molecular-motor-based devices. The sliding velocity as used in this paper has been determined on glass coverslips covered with the same coating as the QCM crystals; any variation in sliding velocities compared to those reported elsewhere is due to the protein preparation.

Two, completely different types of materials, according to their viscoelastic properties, have been used for the motility experiments. A schematic representation of the viscoelastic properties of the materials throughout the motility assay is presented in Figure 3. First, the TMCS-coated substrate is rigid, thus allowing for the precise analysis using the Sauerbrey

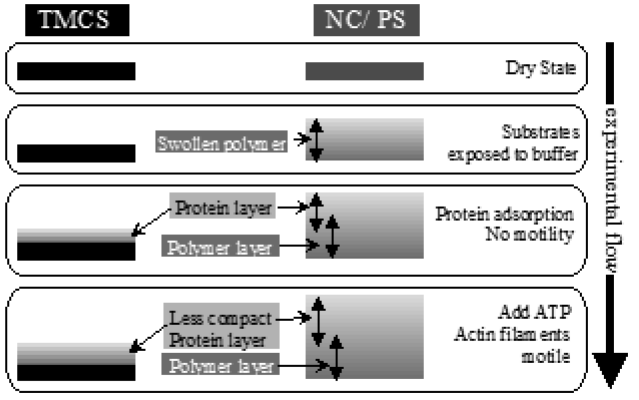

Figure 3. Schematic representation of the evolution of the substrate and protein layers prior and during motility assays processes.

dx.doi.org/10.1021/la302717y | *Langmuir* 2012, 28, 15033−15037

equation. On the other hand, the NC- and PS-coated substrates are relatively rigid in the dry state, but once the substrate is exposed to aqueous solutions, the polymers swell and become more gel-like. The addition of the proteins (HMM and BSA) will make both TMCS and polymer surfaces more comparable in terms of their viscoelastic properties. The final step of the process is the actual motility, where the two different states of the protein motors will manifest themselves. The first is a static state, when no motility occurs and the HMM protein is in a relatively compact confirmation. The second state is dynamic, when motility is occurring; the HMM molecules are constantly switching between two conformations, and the response of the system is given by the (time) average of all molecules.

The changes in both resonance frequency and dissipation do not appear to be correlated strongly with the surface hydrophobicity, estimated by the contact angle (Figure 2), possibly because of the complex correlation between hydrophobicity and protein adsorption and the protein denaturation. Also, in our present experiments, the sliding velocity does not appear to be strongly correlated with the surface hydrophobicity (Figure 4) or with the change in resonance frequency

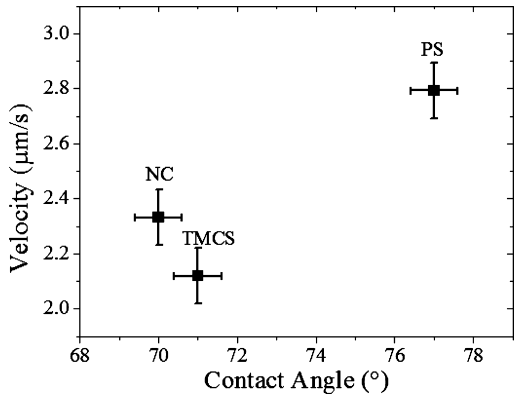

Figure 4. Sliding velocity as a function of the contact angle. The error bars represent one standard deviation.

(Figure 5). However, the velocity, which is a measure of the bioactivity of the protein motors, does appear to be linearly modulated by the apparent dissipation of the film, which is a measure of the gel-like feature of the film (Figure 5). This

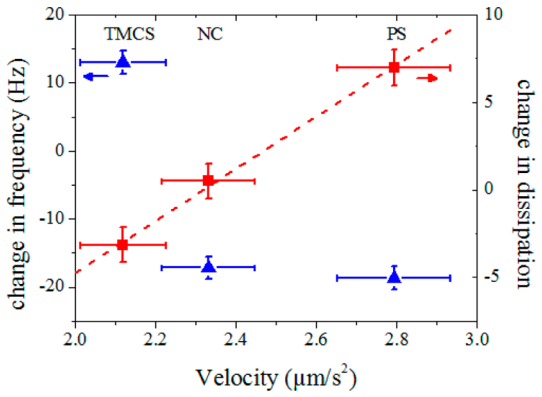

Figure 5. Difference in mass (blue triangles) and dissipation (red squares) between motile and nonmotile filaments as a function of the sliding velocity. Note that the line is a guide for the eye only. The error bars represent one standard deviation. The arrows indicate the relevant axis.

suggests that a host of factors, of which surface hydrophobicity is just one, modulates the mechanical properties of the film, expressed by the apparent dissipation, and this in turn modulates the velocity and the "success" of a motility assay.

The hydrophobicity of the surface coatings, that is, TMCS, NC, or PS, measured prior to the immobilization of the motor proteins (Table 1) plays an essential but also complex role in the adsorption and bioactivity of the surface-immobilized proteins, as witnessed by our previous studies of motility on rigid[53] and polymeric[34] surfaces. However, our previous contributions[34,44,53] that used QCM to study actomyosin motility on surfaces revealed important differences between the behavior of molecular motors on rigid and soft surfaces, respectively, thus suggesting that the nanomechanical properties of the materials also have an important impact on the process of motility on surfaces. In order to study the influence of the rigidity of the film on the actomyosin motility, it is essential that the hydrophobicity or contact angle are as close together as possible.

The surfaces used in this study have initially very different material properties, as TMCS is a molecularly thin film on a rigid substrate that does not absorb water, while NC and PS are polymers that absorb water, in various degrees, and as such start the experiment in a "gel"-like state. However, the adsorption of various proteins on the TMCS-coated surface makes it more similar to a polymer, as can be inferred from the increase in the dissipation on the TMCS-coated crystal due to a change in the viscoelastic properties of the film.

The causality chain of the processes regarding motility on surfaces can be formulated as follows. First, the hydrophobicity of the material, only estimated by the contact angle on the surface, *coupled* with the molecular rigidity of the material, which is high for silicon oxide, and comparatively low for polymers, determine together the water intake in the material exposed to aqueous fluids. A high molecular flexibility and a low hydrophobicity (both on the surface and in the bulk) will result in higher levels of water uptake and consequently a more gel-like structure of the material. Second, it is this gel-like material that is subsequently exposed to the adsorption of the proteins, which is a much slower process due to the much larger mass and volume of the protein compared to the water molecule. While a surface with a high hydrophobicity will result in both higher protein adsorption[54] but also increased levels of protein denaturation,[34] a gel-like, hydrophilic material could induce *both* higher levels of protein adsorption, due to the swelling-induced increase in the specific surface, *and* at the same time low levels of protein denaturation, due to the unhindered state of the protein. The last factor is particularly relevant for molecular motor proteins, as a less molecularly confined and/or less crowded state will allow freer motions of different parts of the molecular structure of the proteins.

4. CONCLUSION

The present contribution explored the relationship between the material properties, as measured by QCM, and the motility characteristics of the actin−myosin system. It has been shown that it is possible to observe differences in the resonance frequency between the motile and nonmotile states associated with the actin filaments. Furthermore, the dissipation of the film correlates well with a continuous parameter of motility, such as sliding velocity. The present study highlights nanomechanical properties of the surface as key modulators of actomyosin motility over a rather narrow range of surface

dx.doi.org/10.1021/la302717y | *Langmuir* 2012, 28, 15033−15037

hydrophobicity where motility is of good quality. These results offer a better understanding of the impact of surfaces on motility for a better design of molecular motors-based devices.

AUTHOR INFORMATION

Corresponding Author

*E-mail: dnicolau@liverpool.ac.uk.

Notes

The authors declare no competing financial interest.

ACKNOWLEDGMENTS

The authors would like to acknowledge funding from the European Union Seventh Framework Programme (FP7/2007-2011) under grant agreement number 228971 (MONAD).

REFERENCES

(1) Sellers, J. R.; Veigel, C. *Curr. Opin. Cell Biol.* **2006**, *18* (1), 68−73.
(2) Sweeney, H. L.; Houdusse, A. *Annu. Rev. Biophys.* **2010**, *39*, 539−557.
(3) Carter, N. J.; Cross, R. A. *Curr. Opin. Cell Biol.* **2006**, *18* (1), 61−67.
(4) Block, S. M. *Biophys. J.* **2007**, *92* (9), 2986−2995.
(5) Hirokawa, N.; Noda, Y.; Tanaka, Y.; Niwa , S. *Nat. Rev. Mol. Cell Biol.* **2009**, *10* (10), 682−696.
(6) Koonce, M. P.; Samsó, M. *Trends Cell Biol.* **2004**, *14* (11), 612−619.
(7) Oiwa, K.; Sakakibara, H. *Curr. Opin. Cell Biol.* **2005**, *17* (1), 98−103.
(8) Huxley, A. F.; Niedergerke, R. *Nature* **1954**, *173* (4412), 971−973.
(9) Huxley, H.; Hanson, J. *Nature* **1954**, *173* (4412), 973−976.
(10) Sheetz, M. P.; Spudich, J. A. *Nature* **1983**, *303* (5912), 31−35.
(11) Spudich, J. A.; Kron, S. J.; Sheetz, M. P. *Nature* **1985**, *315* (6020), 584−586.
(12) Kron, S. J.; Spudich, J. A. *Proc. Natl. Acad. Sci. U.S.A.* **1986**, *83* (17), 6272−6276.
(13) Toyoshima, Y. Y.; Kron, S. J.; Spudich, J. A. *Proc. Natl. Acad. Sci. U.S.A.* **1990**, *87*, 7130−7134.
(14) Harada, Y.; Noguchi, A.; Kishino, A.; Yanagida, T. *Nature* **1987**, *326* (6115), 805−808.
(15) Uyeda, T. Q. P.; Abramson, P. D.; Spudich, J. A. *Proc. Natl. Acad. Sci. U.S.A.* **1996**, *93* (9), 4459−4464.
(16) Hess, H. *Annu. Rev. Biomed. Eng.* **2011**, *13*, 429−450.
(17) Bakewell, D. J. G.; Nicolau, D. V. *Aust. J. Chem.* **2007**, *60* (5), 314−332.
(18) Martinez-Neira, R.; Kekic, M.; Nicolau, D.; dos Remedios, C. G. *Biosens. Bioelectron.* **2005**, *20* (7), 1428−1432.
(19) Bull, J. L.; Hunt, A. J.; Meyhofer, E. *Biomed. Microdevices* **2005**, *7* (1), 21−33.
(20) Limberis, L.; Stewart, R. J. *Nanotechnology* **2000**, *11* (2), 47−51.
(21) Suzuki, H.; Yamada, A.; Oiwa, K.; Nakayama, H.; Mashiko, S. *Biophys. J.* **1997**, *72* (5), 1997−2001.
(22) Nicolau, D. V.; Suzuki, H.; Mashiko, S.; Taguchi, T.; Yoshikawa, S. *Biophys. J.* **1999**, *77* (2), 1126−1134.
(23) Riveline, D.; Ott, A.; Julicher, F.; Winkelmann, D. A.; Cardoso, O.; Lacapere, J. J.; Magnusdottir, S.; Viovy, J. L.; Gorre-Talini, L.; Prost, J. *Eur. Biophys. J. Biophys.* **1998**, *27* (4), 403−408.
(24) Clemmens, J.; Hess, H.; Howard, J.; Vogel, V. *Langmuir* **2003**, *19* (5), 1738−1744.
(25) Clemmens, J.; Hess, H.; Lipscomb, R.; Hanein, Y.; Bohringer, K. F.; Matzke, C. M.; Bachand, G. D.; Bunker, B. C.; Vogel, V. *Langmuir* **2003**, *19* (26), 10967−10974.
(26) Jaber, J. A.; Chase, P. B.; Schlenoff, J. B. *Nano Lett.* **2003**, *3*, 1505−1509.
(27) Moorjani, S. G.; Jia, L.; Jackson, T. N.; Hancock, W. O. *Nano Lett.* **2003**, *3* (5), 633−637.
(28) Clemmens, J.; Hess, H.; Doot, R.; Matzke, C. M.; Bachand, G. D.; Vogel, V. *Lab Chip* **2004**, *4* (2), 83−86.
(29) Bunk, R.; Klinth, J.; Montelius, L.; Nicholls, I. A.; Omling, P.; Tagerud, S.; Mansson, A. *Biochem. Biophys. Res. Commun.* **2003**, *301*, 783−788.
(30) Hiratsuka, Y.; Tada, T.; Oiwa, K.; Kanayama, T.; Uyeda, T. Q. P. *Biophys. J.* **2001**, *81* (3), 1555−1561.
(31) Bunk, R.; Klinth, J.; Rosengren, J.; Nicholls, I.; Tagerud, S.; Omling, P.; Mansson, A.; Montelius, L. *Microelectron. Eng.* **2003**, *67*−*8*, 899−904.
(32) Bunk, R.; Sundberg, M.; Mansson, A.; Nicholls, I. A.; Omling, P.; Tagerud, S.; Montelius, L. *Nanotechnology* **2005**, *16*, 710−717.
(33) Sundberg, M.; Rosengren, J. P.; Bunk, R.; Lindahl, J.; Nicholls, I. A.; Tagerud, S.; Omling, P.; Montelius, L.; Mansson, A. *Anal. Biochem.* **2003**, *323* (1), 127−138.
(34) Nicolau, D. V.; Solana, G.; Kekic, M.; Fulga, F.; Mahanivong, C.; Wright, J.; Ivanova, E. P.; dos Remedios, C. G. *Langmuir* **2007**, *23*, 10846−10854.
(35) Albet-Torres, N.; O'Mahony, J.; Charlton, C.; Balaz, M.; Lisboa, P.; Aastrup, T.; Mansson, A.; Nicholls, I. A. *Langmuir* **2007**, *23*, 11147−11156.
(36) Sauerbrey, G. *Z. Phys.* **1959**, *155* (2), 206−222.
(37) Mason, W. P. *Piezoelectric Crystals and Their Applications to Ultrasonics*; Van Nostand: Princeton, NJ, 1948.
(38) Johannsmann, D. *Macromol. Chem. Phys.* **1999**, *200*, 501−513.
(39) Banda, L.; Alcoutlabi, M.; McKenna, G. B. *J. Polym. Sci., Part B: Polym. Phys.* **2006**, *44*, 801−814.
(40) Granstaff, V. E.; Martin, S. J. *J. Appl. Phys.* **1994**, *75* (3), 1319−1329.
(41) Martin, S. J.; Frye, G. C.; Senturia, S. D. *Anal. Chem.* **1994**, *66* (14), 2201−2219.
(42) Shen, D. Z.; Huang, M. H.; Chow, L. M.; Yang, M. S. *Sens. Actuators, B* **2001**, *77* (3), 664−670.
(43) Yang, M. S.; Thompson, M. *Anal. Chem.* **1993**, *65* (9), 1158−1168.
(44) Albet-Torres, N.; Gunnarsson, A.; Persson, M.; Balaz, M.; Höök, F.; Månsson, A. *Soft Matter* **2010**, *6* (14), 3211−3219.
(45) Balaz, M.; Sundberg, M.; Persson, M.; Kvassman, J.; Månsson, A. *Biochemistry* **2007**, *46* (24), 7233−7251.
(46) Mansson, A.; Balaz, M.; Albet-Torres, N.; Rosengren, K. J. *Front. Biosci., Landmark Ed.* **2008**, *13*, 5732−5754.
(47) Sundberg, M.; Balaz, M.; Bunk, R.; Rosengren-Holmberg, J. P.; Montelius, L.; Nicholls, I. A.; Omling, P.; Tagerud, S.; Mansson, A. *Langmuir* **2006**, *22* (17), 7302−7312.
(48) Chinthalapudi, K.; Taft, M. H.; Martin, R.; Heissler, S. M.; Preller, M.; Hartmann, F. K.; Brandstaetter, H.; Kendrick-Jones, J.; Tsiavaliaris, G.; Gutzeit, H. O.; Fedorov, R.; Buss, F.; Knölker, H. J.; Coluccio, L. M.; Manstein, D. J. *J. Biol. Chem.* **2011**, *286* (34), 29700−29708.
(49) Heissler, S. M.; Manstein, D. J. *J. Biol. Chem.* **2011**, *286* (24), 21191−21202.
(50) Nicolau, D. V.; Nicolau, D. V., Jr.; Solana, G.; Hanson, K. L.; Filipponi, L.; Wang, L. S.; Lee, A. P. *Microelectron. Eng.* **2006**, *83* (4−9), 1582−1588.
(51) Cheng, C. I.; Chang, Y. P.; Chu, Y. H. *Chem. Soc. Rev.* **2012**, *41* (5), 1947−1971.
(52) Saitakis, M.; Gizeli, E. *Cell. Mol. Life Sci.* **2012**, *69* (3), 357−371.
(53) Persson, M.; Albet-Torres, N.; Ionov, L.; Sundberg, M.; Höök, F.; Diez, S.; Månsson, A.; Balaz, M. *Langmuir* **2010**, *26* (12), 9927−9936.
(54) Vasina, E. N.; Paszek, E.; Nicolau, D. V. *Lab Chip* **2009**, *9* (7), 891−900.